

# Superconducting critical current of a single $\text{Cu}_2\text{O}_4$ plane in a $\text{Bi}_2\text{Sr}_2\text{CaCu}_2\text{O}_{8+x}$ single crystal

L. X. You,\* A. Yurgens, and D. Winkler

*Quantum Device Physics Laboratory, Department of Microtechnology and Nanoscience, Chalmers University of Technology, SE-412 96 Göteborg, Sweden*

(Received 2 July 2004; revised manuscript received 25 January 2005; published 7 June 2005)

By feeding current into the topmost  $\text{Cu}_2\text{O}_4$  layer of a mesa etched into the surface of a  $\text{Bi}_2\text{Sr}_2\text{CaCu}_2\text{O}_{8+x}$  (BSCCO) single crystal, we measured its superconducting critical value from a sharp upturn or break in the current-voltage characteristics of the mesa. From this, we estimate the sheet critical current density of a single  $\text{Cu}_2\text{O}_4$  plane to be  $\sim 0.3\text{--}0.7$  A/cm at 4.5 K, corresponding to the bulk current density of  $2\text{--}5$  MA/cm<sup>2</sup>. These values are among the largest ever measured for BSCCO single crystals, thin films and tapes, and we argue that they represent the true intrinsic values of the material.

DOI: 10.1103/PhysRevB.71.224501

PACS number(s): 74.25.Sv, 74.50.+r, 74.25.Fy, 74.72.Hs

## I. INTRODUCTION

The naturally layered structure along the  $c$  axis of high-temperature superconductors (HTSs) is an important feature that accounts for the large anisotropy of transport and superconducting properties along and perpendicular to the layers. It is well established that the  $c$ -axis transport results from sequential *tunneling* of charge carriers between the  $\text{Cu}_2\text{O}_4$  (Cu–O) planes that turns into Josephson tunneling below the superconducting critical temperature  $T_c$ . This intrinsic Josephson effect was first discovered about ten years ago<sup>1,2</sup> and has been a subject of many studies since then.<sup>3</sup> It is worth noting that no other examples of Josephson tunneling that occurred in entirely single-crystalline media had been known until the discovery.

To justify commercial use of HTS materials in power applications, the critical current densities of prototype cables should be sufficiently high. The bottleneck of HTS-cable performance is assumed to be in poor intergrain connectivity and bad  $c$ -axis conductivity of the material while the in-plane ( $ab$ ) superconducting critical current densities  $J_{c\parallel ab}$  are acceptably high. Both from a fundamental and an applied point of view, it is important to know whether the measured  $J_{c\parallel ab}$  reflects the genuine properties of the material. In most cases, however, the measurements of  $J_{c\parallel ab}$  have been made on relatively large single crystals and thin films. Those might include stacking faults and grain boundaries which obviously limit the observed  $J_{c\parallel ab}$ . Moreover, to correctly measure  $J_{c\parallel ab}$  for materials with the highest anisotropy, such as  $\text{Bi}_2\text{Sr}_2\text{CaCu}_2\text{O}_{8+x}$  (BSCCO), the current should be injected uniformly in every Cu–O plane across the thickness of the single crystal, while any imbalance will lead to redistribution of current between the planes thus involving the out-of-plane ( $c$ -axis) properties.

In this paper, we present a method of measuring  $J_{c\parallel ab}$  of a *single* Cu–O plane in BSCCO utilizing its layered nature and the presence of the intrinsic Josephson effect.<sup>1,2</sup> We use an extended intrinsic Josephson junction<sup>4</sup> (IJJ) and a nonuniform current bias<sup>5</sup> flowing along the topmost electrode of the junction, i.e., along the single Cu–O plane. A distinct feature of the current-voltage ( $I$ - $V$ ) characteristic of the IJJ marks the moment when this current exceeds its superconducting critical value within the Cu–O plane.

The thickness of one intrinsic Josephson junction in BSCCO is only 1.5 nm, which explains why it is difficult to isolate and study such a single junction. As a result, most results on IJJs were obtained from stacks (mesas) containing many IJJs. There were a few successful attempts of making stacks enclosing a single IJJ, either by accident<sup>6</sup> or by using a tricky etching technique involving *in situ* monitoring of the resulting current-voltage ( $I$ - $V$ ) characteristics of the stack.<sup>7</sup>

By precisely controlling the fabrication parameters, we successfully made stacks with a low number of IJJs, as well as a single intrinsic Josephson junction (SIJJ).<sup>8,9</sup> In our four-probe measurements of a SIJJ, a steep upturn of the quasiparticle branch occurs at a relatively low bias current when the in-plane current reaches the critical value for a single Cu–O plane. From this we can estimate the sheet critical current density of a single Cu–O plane to be  $\sim 0.3\text{--}0.7$  A/cm at 4.5 K. A back bending of the quasiparticle branch followed by a reentrance to the zero-voltage state is also observed and is explained by significant Joule heating at higher bias currents.

In stacks with many junctions, the transition of the topmost layer is seen as a break in the  $I$ - $V$  characteristics, most clearly in the last quasiparticle branch. Observed by several groups, these breaks were not fully understood until now.

## II. SAMPLE PREPARATION

The samples were made from nearly optimally doped BSCCO single crystals. The stacks of IJJs were formed by photolithography and Ar-ion etching in two steps.

First, a single crystal is cleaved and a thin film of gold (20–30 nm) is deposited in order to protect the surface from deterioration during photolithography patterning. Then, by controlling the process parameters,<sup>8,9</sup> a stack of a certain height  $h \sim 10$  nm is formed on a surface of the single crystal by Ar-ion etching. For the same ion-beam parameters, the height depends linearly on the etching time and thus can be easily controlled. At last, during the second Ar-ion etching, a gap between the contacts is formed in the middle of the stack. The gap is etched to a specified depth  $d = h - n \times 1.5$  nm, where  $n$  represents the number of junctions below the gap in the stack. The height  $h$  and the depth  $d$  could also

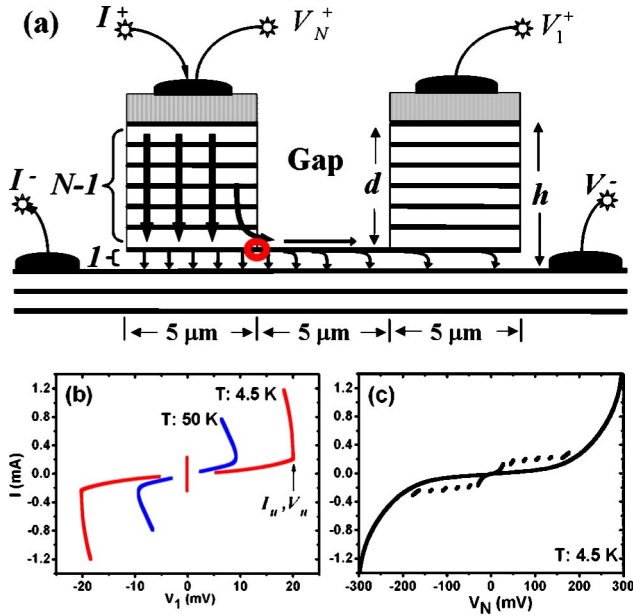


FIG. 1. (Color online.) (a) Schematic view of the sample with a SIJJ. The circle marks the place where the highest in-plane current flows; (b) four-probe  $I$ - $V$  curves of a single intrinsic Josephson junction with the voltage measured between  $V_1^+$  and  $V^-$  contacts at two temperatures  $T=4.5$  and  $50 \text{ K}$ ; (c) three-probe  $I$ - $V$  curves of the sample with the voltage measured between  $V_N^+$  and  $V^-$  at  $4.5 \text{ K}$ . Note the voltage jumps corresponding to seven junctions (the SIJJ in series with the junctions underneath the current contact).

be verified to the accuracy of one junction ( $\sim 1.5 \text{ nm}$ ) by measuring the  $I$ - $V$  characteristics of the resulting sample at low temperature.<sup>10</sup>

In the end, the overall stack acquires a U-shaped form [see Fig. 1(a)], with two smaller stacks under the current and potential contacts sitting on top of the common pedestal which is only  $1.5 \text{ nm}$  high. Following this technique, we can make a specified number of effective junctions enclosed in the base stack, including the most interesting case of SIJJ in this paper. An account of the detailed fabrication process is published elsewhere.<sup>8,9</sup>

In four-terminal measurements [Fig. 1(a)], two contacts are on the top of the SIJJ while two other contacts are placed somewhere else on the crystal surface outside the original stack.<sup>11</sup> With voltage measured between  $V_1^+$  and  $V^-$ , only the effective single junction in the base is registered [Fig. 1(b)]. However, the extra 5–6 junctions underneath the contact stacks may have a profound effect on the resulting  $I$ - $V$  curve due to Joule heating, as will be discussed below.

### III. SURFACE TOPOGRAPHY

In the suggested method, it is important that the top electrode of the SIJJ is spatially uniform. One may argue, however, that the Ar-ion etching is not sufficiently homogeneous to produce an atomically smooth surface after the etching.

To examine the surface roughness before and after the etching, atomic force microscopy (AFM) is used. Figure 2

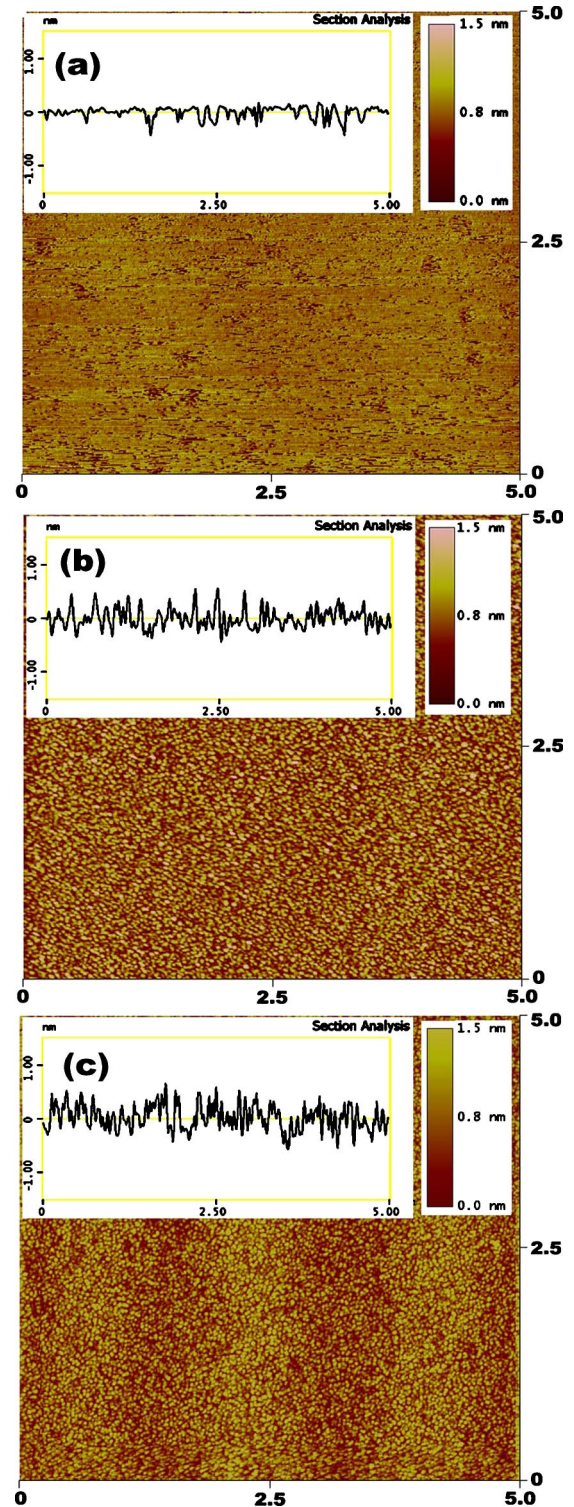


FIG. 2. (Color online) AFM analysis of BSCCO surface. (a) A freshly cleaved BSCCO surface with an r.m.s. surface roughness of  $0.20 \text{ nm}$ . (b) The surface outside the mesa with an r.m.s. surface roughness of  $0.26 \text{ nm}$ . (c) BSCCO surface in the middle of the mesa ("gap" region) with an rms surface roughness of  $0.38 \text{ nm}$ . The imaged areas are  $5 \times 5 \mu\text{m}^2$ .

shows the BSCCO surface of a sample at the gap region and outside of the mesa, as well as a freshly cleaved crystal surface for comparison.

It is seen that the rms surface roughness of the etched areas is 0.38 nm at most, to be compared to the roughness of the freshly cleaved surface of 0.20 nm. All these values are less than one third of the thickness of the insulating barrier layers between the Cu–O layers (1.2 nm), which means that the etched surface of BSCCO is flat enough for forming a sufficiently uniform top electrode of SIJJ. The high degree of smoothness of the etched area is partly due to the low ion energy (230 eV) and beam intensity ( $7 \times 10^{14} \text{ s}^{-1} \text{ cm}^{-1}$  or  $0.11 \text{ mA/cm}^2$ ) used throughout the etching process.<sup>12</sup>

#### IV. LOW-CURRENT MEASUREMENTS

All the measurements were carried out in a liquid-helium Dewar. The temperature was changed by placing the specimen in cold He vapor above the liquid-He level.

Figure 1(b) shows a typical  $I$ - $V$  curve of a SIJJ at two temperatures where only one quasiparticle branch is seen. A sharp upturn of the quasiparticle branch is observed at about  $V_u=20 \text{ mV}$  at 4.5 K and bias current  $I_u=0.22 \text{ mA}$  denoted by the arrow in Fig. 1(b). A three-probe measurement is also shown in Fig. 1(c) for comparison, where all IJJs situated in the small stack under the current contact and the SIJJ are seen in series.

By examining the current flow through the structure, we argue that the sharp upturn at the  $(V_u, I_u)$  point is due to the in-plane current flowing along the topmost Cu–O plane of the SIJJ exceeding its critical value. Indeed, when the bias current is spatially nonuniform for the SIJJ, i.e., is applied to one end, it first tends to distribute itself over the whole surface of the SIJJ's top electrode. This means that a finite in-plane superconducting current must flow between the current and potential electrodes, as depicted in Fig. 1(a). If it exceeds the critical value, the top electrode becomes resistive thus breaking the connection between the two parts of the junction. Then, the current will be redistributed between these parts, dependent on their particular  $c$ -axis resistances and the resistance of the "bridge" between them. The corresponding voltage measured at the potential contact will be a function of all the nonlinear resistances involved.

The highest in-plane current density is expected to be in the place where the small mesa under the bias electrode ends and where the bias current starts to spread itself along the top electrode of the SIJJ [marked by a circle in Fig. 1(a)]. Each electrode (the small mesa  $\sim 5 \times 5 \mu\text{m}^2$ ) occupies about one third of the total area of the SIJJ ( $\sim 15 \times 5 \mu\text{m}^2$ ). This means that initially, when the top electrode of the SIJJ is still superconducting, about one third of the bias current passes along the  $c$  axis directly through the area under the current-bias contact. The remaining two thirds will flow nonuniformly through the rest of the junction area, which in turn means that the maximum value of the  $ab$ -plane superconducting current is roughly equal to two thirds of the total bias current. The (sheet) critical current density of a single Cu–O plane can be estimated to be about  $0.3 \text{ A/cm}$  at 4.5 K after dividing  $2/3I_u$  by the width of the SIJJ ( $5 \mu\text{m}$ ). To be able to compare this value to the published bulk critical current densities, we need to take into account the total thickness of SIJJ (1.5 nm). Hence, the (bulk) in-plane critical current density

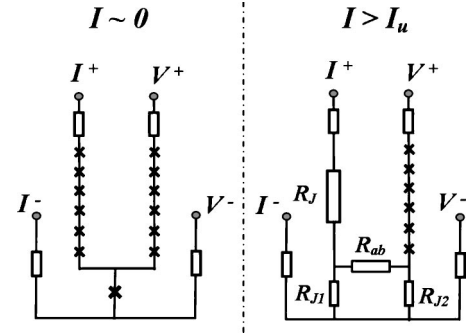


FIG. 3. A simple equivalent circuit of the junction stack in four-probe measurement. The crosses schematically show the intrinsic Josephson junctions. Small unmarked resistors represent resistance of connecting wires and the contact resistances. In the quasiparticle-tunneling state, the junctions are represented by the corresponding nonhysteretic and nonlinear resistances.

of BSCCO can be estimated to be about  $2.0 \text{ MA/cm}^2$ . Although being quite reasonable, this value is among the largest ever observed in other  $J_{c\parallel ab}$  measurements.<sup>13–20</sup>

Further proof of the method was obtained from another sample ( $18 \times 3 \mu\text{m}^2$ ) with two top electrodes of different sizes ( $S_L: 9 \times 3 \mu\text{m}^2$  and  $S_R: 5 \times 3 \mu\text{m}^2$ ). By passing the current through two different top electrodes, two different values of  $I_u$  ( $I_{u:L}=0.45 \text{ mA}$  and  $I_{u:R}=0.31 \text{ mA}$ ) for the sharp upturn structure were observed in similar  $I$ - $V$  curves. However, considering the sizes of the electrodes, the same critical current  $I_{c\parallel ab}=0.22 \text{ mA}$  of a single Cu–O plane was obtained. The corresponding sheet critical current density of  $0.7 \text{ A/cm}$  is higher than the value for the former sample, which can be explained by the spread of  $J_c$  from crystal to crystal.

A simple equivalent circuit shown in Fig. 3 can be used to highlight the situation qualitatively. We model the junction resistances in the  $c$ -axis direction by nonlinear  $V_j(I)$  functions.  $V_j(I)$  per junction is deduced from the measured  $V(I)$  dependence corresponding to the last quasiparticle branch in Fig. 1(c) by dividing the voltage by the number of junctions in the whole mesa.

In order to model the dynamics of the current flow through the SIJJ, we assume quite arbitrarily the following form of the voltage drop across the  $ab$  plane at the bridge between the two regions:

$$V_{ab}(I) = R_{ab}I \left[ 1 + \exp\left(\frac{I_c - I}{\delta I}\right) \right]^{-1}. \quad (1)$$

$V_{ab}(I)$  of Eq. (1) simulates a transition from the superconducting to the normal state of the top electrode of SIJJ. We see that  $V_{ab}(I)$  is exponentially small when  $I < I_c$  ("superconducting state") and is finite and Ohmic,  $V_{ab}(I) = R_{ab}I$ , when  $I > I_c$  (normal state with the resistance  $R_{ab}$ ).  $\delta I$  represents the "rounding" of the transition ( $\delta I \ll I_c$ ).

The equivalent circuit shown in Fig. 3 can further be used to qualitatively simulate the resulting current-voltage curve at small bias. It is shown in Fig. 4 for the parameters  $\delta I = 0.003 \text{ mA}$ ,  $I_c = 0.15 \text{ mA}$ , and  $R_{ab} = 2 \text{ k}\Omega$ .  $R_{ab}$  corresponds to the sheet resistance of a single Cu–O plane taking the  $ab$  resistivity to be  $300 \mu\Omega/\text{cm}$ .<sup>21</sup>

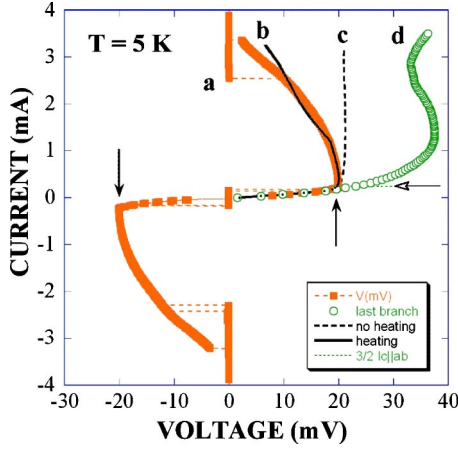


FIG. 4. (Color online.) (a) The four-probe current-voltage curve of the single intrinsic Josephson junction at high bias; (b), (c) simulated  $I$ - $V$  curves using the simple equivalent circuit depicted in Fig. 3. The horizontal dashed line and the hollow arrow show the value of the bias current corresponding to  $1.5I_{c|lab}$ . The vertical arrows mark the sharp upturn of the quasiparticle branch; (d)  $I$ - $V$  curve assumed for a single junction when the bias current is uniform. This curve was obtained from the last quasiparticle branch [see Fig. 1(c)] by dividing the voltage by the number of junctions involved.

The dashed line (c) in Fig. 4 mimics the steep upturn of the measured  $I$ - $V$  curve and explains the upturn structure at low bias current qualitatively well. It should also be noted that at the  $(V_u, I_u)$  point where the break and the upturn of the quasiparticle branch is seen, the Joule dissipation and, hence, overheating is quite small and cannot explain these features. Indeed, from Fig. 1(c) it follows that the total dissipation of the whole stack is less than  $50 \mu\text{W}$  at  $I=I_u$ . Using typical values for the thermal resistance,<sup>22</sup>  $40\text{--}70 \text{ K/mW}$ , we judge that the temperature rise should be less than  $4 \text{ K}$ . Moreover, any suggested decrease of the superconducting gap caused by heating should be gradual and the corresponding  $I$ - $V$  feature should not be sharp. However, Joule heating increases with current and gradually becomes visible at higher bias currents, as will be shown below.

## V. HIGH-CURRENT MEASUREMENTS

The simulated  $I$ - $V$  curve in Fig. 4 has no back bending in contrast to what is seen experimentally. In fact, the back bending in the experiment is so large that the corresponding voltage eventually becomes zero at a high current. We think that both the back-bending and the current-induced zero-voltage state can be qualitatively explained by Joule heating in the region where the current is supplied to the junction.

Indeed, the heat dissipation and, correspondingly, the temperature of the stack progressively increase with the bias current. The temperature dependence of the bridge resistance  $R_{ab}=R_{ab}(T)$  and its critical current  $I_c=I_c(T)$  should then be taken into account. The former increases, while the latter decreases with temperature. Qualitatively, this means that increasing the bias current will result in a reduction of its fraction that is branching off towards the potential electrode. In other words, a smaller current is flowing through  $J_2$  for

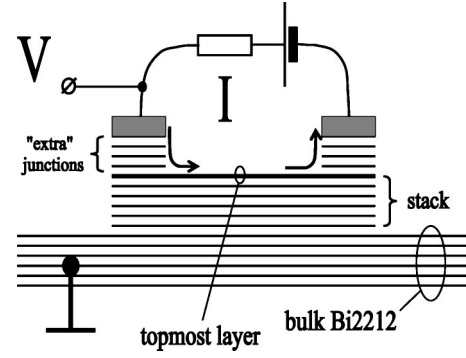


FIG. 5. A simple equivalent circuit of the multi-junction stack in a three-probe measurement when the bias current is fed into the topmost layer of the stack through a few extra junctions under the metallic contacts. The voltage is measured relative to the bulk of the Bi2212 single crystal using another mesa somewhere else on the surface of the crystal.

higher current biases. Even if taking into account the somewhat compensating effect of the nonlinear  $I$ - $V$  characteristic in the  $c$ -axis direction, this can still result in the smaller voltage drop across  $R_{J_2}$ . Eventually, when this current becomes smaller than the retrapping current for  $J_2$ , it will switch into the zero-voltage state.

While the small stack under the current lead is believed to be the main source of heating, numerical simulations were done by including a dependence of  $R_{ab}$  and  $I_{c|lab}$  on the current through  $J_1$ ,  $I_{J_1}$ . The increase of  $R_{ab}(I_{J_1})$  and decrease of  $I_{c|lab}(I_{J_1})$  with temperature could be tested with different dependencies. Curve (b) in Fig. 4 was obtained by assuming linear dependencies. Taking the real energy dissipation into account, i.e., assuming that  $R_{ab}$  and  $I_{c|lab}$  are functions of the product  $I_{J_1}V_{J_1}$  or  $I_{J_1}^2$  and not simply  $I_{J_1}$  did not yield much better fits.

It is worth noting that in order to get back-bending of the  $I$ - $V$  curve using this simple equivalent circuit, it is essential to include the heating effects. No form of nonlinearity in  $V_{ab}(I_{ab})$  could help model the back bending unless we included the dependence  $V_{ab}$  on  $I_{J_1}$ ,  $V_{ab}=V_{ab}(I_{ab}, I_{J_1})$ , as we shortly described above. Curves resembling curve (c) of Fig. 4 could only be obtained otherwise in most cases.

One should not expect quantitatively correct results from these simulations due to the much simplified equivalent circuit used and also due to a somewhat uncertain current distribution in the base crystal below the SIJJ. The plane just below the mesa can switch to the normal state at sufficiently high current as well. Then, the voltage drop will also depend on the geometry of base current and potential contacts along the crystal surface. To take even this into account looks unjustified in view of the simplifications which were used.

## VI. MULTIPLE-JUNCTION STACKS

To see the  $ab$ -plane superconducting transition of a single  $\text{Cu-O}$  plane in higher stacks containing many junctions, we apply a current between the two top electrodes. The voltage on either of the contacts relative to the bulk of the single

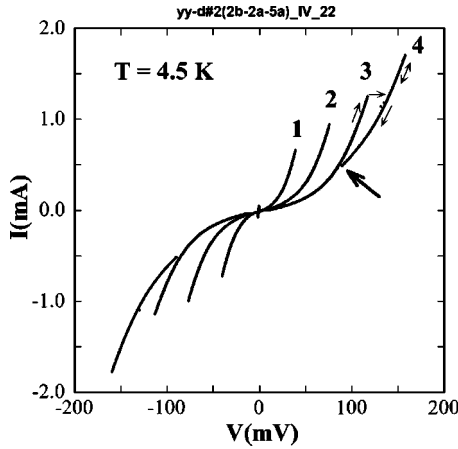


FIG. 6. A current-voltage characteristic of a mesa  $\approx 30 \times 7 \mu\text{m}^2$  in area measured in accordance with schematics shown in Fig. 5. There are three “extra” junctions under each of the contacts seen as three first branches (1–3).<sup>10</sup> The “pedestal” stack contains four junctions ( $I$ - $V$  not shown). The zero-voltage superconducting branch has a much smaller critical current as the topmost “extra” junction is in direct contact to the normal-metal thin film. The thick arrow marks the position of the break corresponding to the superconducting transition of the surface layer when the current through it becomes less than the critical value. Thin arrows indicate current directions for tracing out the hysteresis in the  $I$ - $V$  characteristic.

crystal is then measured versus the applied current, which initially flows through the topmost Cu–O plane of the stack, as is schematically shown in Fig. 5.

In the arrangement without “extra” junctions, no voltage is expected to appear unless the in-plane current along the topmost layer exceeds the critical value. If dealing with the U-shaped mesas with a certain number of “extra” junctions, the voltage will be equal to the voltage across these junctions (plus a small voltage drop across the contact resistance). A feature corresponding to the current-driven transition to the normal state of the topmost layer of the stack is a break of the last quasiparticle branch. The break is also accompanied by the appearance of an extra  $I$ - $V$  branch (see Fig. 6).

The figure shows an  $I$ - $V$  curve of a stack having two contacts on top, with current fed from one stack to the other. The voltage is measured relative to the bulk using another mesa somewhere else on the crystal surface.

There are four quasiparticle branches seen, three having a common point of origin at  $V, I \rightarrow 0$  and the last one having some offset both in voltage and current for the point of origin. The latter is marked by the thick arrow. We argue that this point corresponds to the current-driven superconducting transition of the topmost layer of the stack. Let us describe the whole picture in detail.

The bias current first flows through the small stack (extra junctions) under one contact, then along the topmost electrode and, finally, through the small stack at the other end of the mesa. There are three extra IJJs under each of the contacts on top of the larger stack (pedestal) which contains four junctions. The latter can be seen in the four-probe measurements when the current is directed vertically down to the bulk and the voltage is measured at the second contact of the mesa, exactly as it was done in the case of the single-junction measurements (see above).

When the current exceeds the critical value for the plane, the first junction under the bottom of the extra-junction stack will be divided into two parts and the current redistributes. One part of the current still flows along the plane, and the rest flows downwards through the junction under the bottom of the extra-junction stack. At this moment, however, no voltage appears over that junction (a “hidden” junction) since it is still in the superconducting tunneling state. When the bias current increases, the current through the junction will become larger than its critical current. When this happens, one more extra junction becomes visible in the  $I$ - $V$  curves, see branch “4” in Fig. 6. This means that in the case of ideally equivalent (“extra”) junctions in the small stack, the observed critical current for branch 3 should be larger than the critical current for the previous branches by the value of the in-plane critical current that is branching off towards another electrode.

If the current is set to decrease after that, the hidden junction will not leave the quasiparticle-tunneling state unless the current through it becomes less than the retrapping current. This means that when the *total* bias current becomes less than the sum of the in-plane critical current and the retrapping current of that hidden junction, the system switches back to the state corresponding to branch 3.

Following this scenario, the critical current of the topmost single  $\text{Cu}_2\text{O}_4$  plane corresponds to the current at which branches 3 and 4 cross, see the arrow in Fig. 6, because the retrapping current for a typical IJJ is of the order of a few tens of  $\mu\text{A}$ , i.e., much smaller than the in-plane critical current. Given the width of the stack  $w=7 \mu\text{m}$ , we calculate the sheet critical current density to be  $\approx 0.7 \text{ A/cm}$  corresponding to the bulk in-plane current density of  $4.7 \text{ MA/cm}^2$ .

The superconducting transitions of the second and even third from the top layer can be seen at a high enough current as well. At a high current, however, the Joule heating progressively increases and makes estimations of the corresponding critical current densities somewhat understated.

## VII. DISCUSSION

We have argued that the sheet critical current density of a single Cu–O plane corresponds to the critical current density which would be obtained in a perfect bulk sample. However, the critical current of an isolated superconducting plane in BSCCO should be limited by large thermal fluctuations associated with the two-dimensional (2D) character of the Cu–O planes. Topological defects in the form of 2D vortex-antivortex pairs are likely to arise as a result of these fluctuations, as first suggested by Berezinskii, Kosterlitz, and Thouless (BKT).<sup>23,24</sup> Long enough vortex dipoles can be broken by the transport current and the resulting free 2D vortices will sweep across the superconductor giving rise to dissipation in the system. This scenario leads to a nonlinear behavior of the  $I$ - $V$  characteristics since the number of free vortices obviously depends on the bias current.

We can calculate the sheet critical current density assuming that the in-plane critical current is limited by the BKT mechanism.<sup>25</sup>

$$i_c \left[ \frac{\text{A}}{\text{cm}} \right] = 5.8 \times 10^8 \frac{1}{\lambda_{ab}^2 [\text{\AA}]} \sqrt{\frac{m_{ab}}{m_c}}, \quad (2)$$

where  $\lambda_{ab}$  is the London penetration length;  $m_{ab}$  and  $m_c$  are the effective masses of the superfluid particle for motion in  $ab$  plane and  $c$  direction, respectively.

Taking  $\lambda_{ab} \approx 1800 \text{ \AA}$  and  $m_c/m_{ab} \approx 2 \times 10^5$ , Eq. (2) yields  $I_c \approx 0.4 \text{ A/cm}$  which is very close to the experimental values of 0.3–0.7 A/cm. This is also consistent with early suggestions on BKT-type phase transitions of the layered HTS.<sup>25–27</sup>

Still, the values that we obtain, are among the largest ever observed for BSCCO, both in thin films,<sup>19,20</sup> single crystals,<sup>13–16</sup> and tapes.<sup>17,18</sup> Remarkably, our results are even larger than for whiskers.<sup>15,16</sup> Whiskers are believed to represent the highest quality of BSCCO single crystals, having virtually no stacking faults and grain boundaries. Such extended defects are anticipated to limit the bulk critical current. To the best of our knowledge, however, the largest value of  $J_{c||ab}$  reported for whiskers<sup>15</sup> is 0.5 MA/cm<sup>2</sup>, i.e., a few times smaller than in our experiments and than what can be deduced using Eq. (2). We believe that difficulties to inject current uniformly through the whiskers' cross section may result in a large underestimate of the current density. In most cases, the contacts to the whiskers were applied from the flat in-plane sides causing a highly nonuniform current distribution.<sup>28</sup>

Similar breaks in the  $I$ - $V$  curves to the one presented in Fig. 6 have been seen in several other studies of multijunction stacks of intrinsic Josephson junctions.<sup>29–32</sup> However, these structures were neither commented nor explained.

The position of this feature in current depends, of course, on the size of the stack, the perimeter around it through which the current spreads out over the surface towards another contact on the single crystal, and on superconducting properties of the particular single crystal used. Some geometries are especially favorable for seeing the break in  $I$ - $V$ 's, similar to the case of having one stack placed on top of another one. This is the geometry of our experiment described above while similar arrangements can be found in other published experiments as well.<sup>29,32</sup> In our geometry, the current spreads out over the surface of the base (pedestal) stack through one-fourth of the square perimeter of the small

stack sitting on the top of the former stack (see Figs. 1 and 5). It is clear that in the case of a stand-alone mesa, the current of the break should be four times larger.

The current-induced collapse of superconductivity of the surface layers can have a profound effect on several relatively high-bias tunneling-spectroscopy measurements on the Bi family of high-temperature superconductors. These include the break-junction technique and the intrinsic-tunneling spectroscopic measurements, in particular.

Indeed, the large superconducting energy gap of high-temperature superconductors requires quite high current densities to reach the corresponding gap feature in such experiments. If the current exceeds the critical value for the topmost plane of the base crystal, an extra contribution from the (hidden) junctions in parallel with the in-plane normal-state resistance will add to the measured voltage. How large the false contribution is depends on the particular geometry of experiment but qualitatively, it is anticipated to result in an overestimate of the superconducting energy gap.

## VIII. CONCLUSIONS

The sheet critical current density of a *single* Cu<sub>2</sub>O<sub>4</sub> plane was measured by forcing the current to flow along the topmost electrode of a single intrinsic Josephson junction. The critical current was marked by a steep upturn (break) in the quasiparticle branch of the junction(s) when the superconductivity of the topmost Cu–O layer is destroyed by current. Further increase of the bias current caused a back-bending of the  $I$ - $V$  curve followed by a reentrance to the zero-voltage state. This is explained by progressive increase of Joule-heating at high bias. The values of the sheet critical current 0.3–0.7 A/cm are among the largest values ever reported for BSCCO and are close to theoretically estimated ones assuming a critical-current-limiting BKT nature of 2D superconductivity in copper oxides.

## ACKNOWLEDGMENTS

We thank M. Torstensson and D. Lindberg for technical assistance and T. Claeson and V. Krasnov for fruitful discussions. This work was financed by The Swedish Foundation for Strategic Research (SSF) through the OXIDE program.

\*Electronic address: lixing@mc2.chalmers.se

<sup>1</sup>R. Kleiner, F. Steinmeyer, G. Kunkel, and P. Müller, Phys. Rev. Lett. **68**, 2394 (1992).

<sup>2</sup>R. Kleiner and P. Müller, Phys. Rev. B **49**, 1327 (1992).

<sup>3</sup>A. A. Yurgens, Semicond. Sci. Technol. **13**, R85 (2000).

<sup>4</sup>“Extended” means that the lateral sizes are larger than the so called Josephson penetration depth, see the next reference or M. Tinkham, *Introduction to Superconductivity* (McGraw-Hill, Singapore, 1996).

<sup>5</sup>A. Barone and G. Paternò, *Physics and Applications of the Josephson Effect* (Wiley, New York, 1982).

<sup>6</sup>A. Yurgens, D. Winkler, N. V. Zavaritsky, and T. Claeson, Phys.

Rev. B **53**, R8887 (1996).

<sup>7</sup>A. Yurgens, D. Winkler, T. Claeson, and N. V. Zavaritsky, Appl. Phys. Lett. **70**, 1760 (1997).

<sup>8</sup>L. X. You, P. H. Wu, Z. M. Ji, S. X. Fan, W. W. Xu, L. Kang, C. T. Lin, and B. Liang, Semicond. Sci. Technol. **16**, 1361 (2003).

<sup>9</sup>L. X. You, P. H. Wu, W. W. Xu, Z. M. Ji, and L. Kang, Jpn. J. Appl. Phys., Part 1 **43**, 4163 (2004).

<sup>10</sup>The  $I$ - $V$  curve of IJJs [Fig. 1(c)] usually consists of several branches, each corresponding to one, two, three, and so on, intrinsic Josephson junctions switching to the quasiparticle-tunneling state with increasing bias current. Therefore the height  $h$  can be obtained by multiplying the height of individual IJJ by

- the number of quasiparticle branches of the  $I$ - $V$  characteristic (voltage measured between  $V_N^+$  and  $V^-$ ), i.e.,  $h \sim N \times 1.5$  nm. In the same way, the depth  $d$  can be obtained by multiplying the height of individual IJJ by the number of quasiparticle branches of the  $I$ - $V$  characteristic (voltage measured between  $V_N^+$  and  $V_1^-$ ).
- <sup>11</sup>In fact, other stacks with low contact resistances and much larger areas are used for this purpose. Making contacts to the etched areas can be problematic. The low contact resistances are only possible to reproducibly achieve when the gold thin film is deposited as soon as possible after cleaving the single crystal.
- <sup>12</sup>T. Kamimura, S. Fukumoto, R. Ono, Y. K. Yap, M. Yoshimura, Y. Mori, T. Sasaki, and K. Yoshida, *Opt. Lett.* **27**, 616 (2002).
- <sup>13</sup>T. W. Li, A. A. Menovsky, J. J. M. Franse, and P. H. Kes, *Physica C* **257**, 179 (1996).
- <sup>14</sup>T. Matsushita, T. Hirano, H. Yamato, M. Kiuchi, Y. Nakayama, J. Shimoyama, and K. Kishio, *Semicond. Sci. Technol.* **11**, 925 (1998).
- <sup>15</sup>Yu. I. Latyshev, I. G. Gorlova, A. M. Nikitina, V. U. Antokhina, S. G. Zybtev, N. P. Kukhta, and V. N. Timofeev, *Physica C* **216**, 471 (1993).
- <sup>16</sup>M. Mizutani, H. Uemoto, M. Okabe, and S. Kishida, *Physica C* **392**, 508 (2003).
- <sup>17</sup>E. Flahaut, D. Bourgault, C. E. Bruzek, M. O. Rikel, P. Herrmann, J. L. Soubeyroux, and R. Tournier, *IEEE Trans. Appl. Supercond.* **13**, 3034 (2003).
- <sup>18</sup>K. R. Marken, H. Miao, J. M. Sowa, J. A. Parrell, and S. Hong, *IEEE Trans. Appl. Supercond.* **11**, 3252 (2001).
- <sup>19</sup>K. Yonemitsu, K. Inagaki, T. Ishibashi, S. Kim, K. Lee, and K. Sato, *Physica C* **367**, 414 (2002).
- <sup>20</sup>M. Moriya, Y. Koike, K. Usami, T. Goto, and T. Kobayashi, *Semicond. Sci. Technol.* **15**, 1749 (2002).
- <sup>21</sup>T. Watanabe, T. Fujii, and A. Matsuda, *Phys. Rev. Lett.* **79**, 2113 (1997).
- <sup>22</sup>A. Yurgens, D. Winkler, T. Claeson, S. Ono, and Y. Ando, *Phys. Rev. Lett.* **92**, 259702 (2004).
- <sup>23</sup>V. L. Berezinskii, *Zh. Eksp. Teor. Fiz.* **61**, 1144 (1971) [*Sov. Phys. JETP* **34**, 610 (1972)].
- <sup>24</sup>J. M. Kosterlitz and D. G. Thouless, *J. Phys. C* **6**, 1181 (1973).
- <sup>25</sup>H. J. Jensen and P. Minnhagen, *Phys. Rev. Lett.* **66**, 1630 (1991).
- <sup>26</sup>L. I. Glazman and A. E. Koshelev, *Zh. Eksp. Teor. Fiz.* **97**, 1371 (1990) [*Sov. Phys. JETP* **70**, 774 (1990)].
- <sup>27</sup>S. N. Artemenko and A. N. Kruglov, *Phys. Lett. A* **143**, 485 (1990).
- <sup>28</sup>R. Busch, G. Ries, H. Werthner, G. Kreiselmeyer, and G. Saemann-Ischenko, *Phys. Rev. Lett.* **69**, 522 (1992).
- <sup>29</sup>Y.-J. Doh, H. J. Lee, and H. S. Chang, *Phys. Rev. B* **61**, 3620 (2000).
- <sup>30</sup>A. Irie, S. Heim, S. Schromm, M. Moßle, T. Nachtrab, M. Gódo, R. Kleiner, P. Müller, and G. Oya, *Phys. Rev. B* **62**, 6681 (2000).
- <sup>31</sup>A. Saito, H. Ishida, K. Hamasaki, A. Irie, and G. Oya, *Appl. Phys. Lett.* **85**, 1196 (2004).
- <sup>32</sup>V. M. Krasnov, *Phys. Rev. B* **65**, 140504(R) (2002).